

Near threshold η production in proton-proton collisions

M. Batinić, A. Švarc^{a,1} and T.-S. H. Lee^{b,1}

^aRudjer Bošković Institute, Zagreb, Croatia

^bPhysics Division, Argonne National Laboratory, IL 60439, USA

Abstract

The total cross section for the near threshold η production in proton-proton collisions has been investigated with the assumption that the production mechanism is due to the emission of a meson $x(\pi, \eta, \sigma)$ from one of the nucleons followed by a $xN \rightarrow \eta N$ transition on the second one. The $xN \rightarrow \eta N$ amplitudes are generated from the unitary multi-channel multi-resonance model which has recently been constructed in analyzing the πN scattering and $\pi N \rightarrow \eta N$ reaction. The initial and final pp distortions are calculated from a coupled-channel πNN model which describes the NN scattering data up to about 2 GeV. With the $x - NN$ vertex functions taken from the Bonn potential, the predicted total cross sections of threshold $pp \rightarrow \eta pp$ reaction are in good agreement with the data. In contrast to previous works, we find that the η -exchange plays an important role. The effect of the two-pion exchange, simulated by σ - exchange, is found to be significant but not as dominant as the vector meson-exchange introduced in previous works.

The η production in proton-proton collisions has attracted a lot of interest in the past decade. A theoretical understanding of this two-nucleon process near the production threshold is needed for exploring the $N^*(S_{11}(1535))$ dy-

¹ Partially supported by US-CRO contract JF 221

namics in nuclear medium, possible existence of η -nucleus bound states, and the possibility of using η to reveal the properties of high-density nuclear matter created in relativistic heavy-ion collisions. All of the existing theoretical works[1–5] on this reaction were based on the assumption that the basic mechanism of $NN \rightarrow \eta NN$ reaction is the emission of a meson $x(\pi, \eta, \rho, \dots)$ from one of the nucleons followed by a $xN \rightarrow \eta N$ transition, as illustrated in Fig.1. Clearly, an accurate assessment of this meson-exchange model depends heavily on the accuracy of the employed $xN \rightarrow \eta N$ amplitudes, treatment of the propagation of the exchanged mesons, and the meson– NN vertex functions. Furthermore, the initial and final NN interactions must be accounted for by using realistic NN models. In this work, we investigate all these problems by making use of the recent advance in constructing the $xN \rightarrow \pi N$ amplitudes[6,7] and the knowledge we have learned from previous studies of meson-exchange models[8,9] of nucleon-nucleon interactions.

A common feature of the previous investigations[1–5] of the threshold $pp \rightarrow \eta pp$ reaction is that the ηN channel is only due to the decay of the $N^*(S_{11})$ resonance and the agreement with the data is obtained only when the sub-threshold exchange of vector mesons is introduced. The predicted results thus depend heavily on how the assumptions were made to determine the vector meson coupling constants associated with the decay of the $N^*(S_{11})$ resonance. In Refs.[1–3,5], the vector meson dominance model(VDM) is used to determine the $N^*(S_{11}) - \rho N$ coupling from the branching ratio $\Gamma(N^* \rightarrow \gamma N)/\Gamma(N^* \rightarrow \pi N) = 0.013 \pm 0.004$ [1]. In Ref.[4], this ρ coupling constants is directly determined from the $N^*(S_{11}) \rightarrow \rho N$ decay width listed by the Particle Data Group[10]. The ω exchange is also introduced in Ref.[4] by assuming that its coupling with the N^* relative to that to the nucleon has the same value as for the pion; i.e. $g_{NN^*\omega}/g_{NN\omega} = g_{NN^*\pi}/g_{NN\omega}$. These differences in choosing the vector meson coupling constants had led to conflicting conclusions between these earlier investigations. The ρ -exchange was found to be dominant

in Refs.[1–3], while the importance of the ω -exchange was stressed in Ref.[4].

In this work, we will not follow these earlier approaches to consider the possible contributions from vector mesons exchanges. Instead, our main objective is to examine the extent to which the threshold $pp \rightarrow \eta pp$ data can be understood from the π and η exchange which can be calculated with no adjustable parameters. This will be accomplished by using the $\pi N \rightarrow \eta N$ and ηN elastic amplitudes generated from the recently constructed unitary multi-channel, multi-resonance model of Ref.[6,7] and the $\pi - NN$ and $\eta - NN$ vertex functions taken from the Bonn potential[8]. We then estimate the importance of the two- π exchange by assuming that the fictitious third-channel in the employed unitary multi-channel, multi-resonance model is a σN channel with σ identified with the one in the same Bonn potential. Another important feature of our calculation is the πNN model developed in Ref. [9] which accounts for the initial and final pp distortions. This model was constructed to give a good description of NN scattering up to about 2 GeV. The use of such a realistic model is essential for calculating the initial pp distortion in the considered rather high energies $E_L \sim 1.3$ GeV. The final pp distortion is also calculated from the same model which is as accurate as the Paris potential at low energies, as discussed in Ref.[9].

Table I

x	$\frac{g_{xNN}^2}{4\pi}$	Λ_x (MeV/c)
π	14.9	1300
η	2.0	1500
σ	8.7	2000

In terms of the kinematical variables in Fig.1, the expression for the spin-averaged total cross section of $pp \rightarrow pp\eta$ reaction can be written as the fol-

lowing form :

$$\sigma_{tot} = \int dq d\Omega_\eta d\Omega_1 \frac{d^5\sigma}{dq d\Omega_\eta d\Omega_1}, \quad (1)$$

with

$$\frac{d^5\sigma}{dq d\Omega_\eta d\Omega_1} = \frac{2m^4 q^2 p_1^2}{(2\pi)^5 E_\eta (p_1 E_2 - E_1 \vec{p}_1 \cdot \hat{p}_2)} \frac{1}{\sqrt{(p_b \cdot p_t)^2 - m^4}} \left[\frac{1}{4} \sum_{spins} |M_{fi}|^2 \right]. \quad (2)$$

with p_b and p_t being beam and target four momenta, and p_1 and p_2 (E_1 and E_2) are the final nucleon three c.m. momenta and energy. E_η is the η -c.m. energy. The transition matrix element is defined by

$$M_{fi} = \langle \chi_f^{(-)} | M^0 | \chi_i^{(+)} \rangle, \quad (3)$$

where $\chi_f^{(-)}$ and $\chi_i^{(+)}$ are respectively the final and initial pp scattering wave-functions generated from the πNN model of Ref.[9]. The production operator M^0 is

$$M^0 = \sum_{x=\pi,\eta,\sigma} M^{x,0}, \quad (4)$$

where the contribution from each exchanged meson x is defined by the following plane-wave invariant matrix element

$$M^{x,0} = \left\{ \begin{array}{l} \left[\bar{u}(p_1, s_1) (A_x + \not{q} B_x) u(p_b, s_b) \frac{i}{p_x^2 - m_x^2} \bar{u}(p_2, s_2) V_{xNN}(p_x^2) u(p_t, s_t) \right] \\ - [1 \leftrightarrow 2] \\ - \{b \leftrightarrow t\}. \end{array} \right. \quad (5)$$

Here, A_x and B_x are the $xN \rightarrow \eta N$ invariant functions generated from the unitary multi-channel, multi-resonance model of Ref.[6,7]. It is worthwhile to note that the range of the constructed production operator depends on how the momentum-transfer variable p_x in Eq.(5) is evaluated. In this work, we follow the usual meson-exchange model of nuclear force[8,9] to set all nucleons

on their mass-shell to choose $p_x^2 = (p_t - p_2)^2 = (E_N(\vec{p}_t) - E_N(\vec{p}_2))^2 - (\vec{p}_t - \vec{p}_2)^2$. The resulting operator is always finite range in coordinate space. This is very different from the treatment of Ref.[1,2,5]. These authors obtained an oscillating one-pion-exchange which is of infinite range in coordinate space.

The $x - NN$ vertex function in Eq.(5) is parameterized as a monopole form

$$V_{xNN} = g_{xNN} \frac{\Lambda_x^2 - m_x^2}{\Lambda_x^2 - p_x^2}, \quad (6)$$

The parameters Λ_x and g_{xNN} used in this work are taken from the Bonn potential[8] and is given in Table 1(from Table A.3 of Ref.[8]).

We first examine the distortion effects. In Fig.2, we display the distortion factors calculated from the following expressions:

$$f_{ISI} = \frac{\int N | \langle \chi_f^{(-)} | M^0 | \chi_i^{(+)} \rangle |^2 dX}{\int N | \langle \chi_f^{(-)} | M^0 | \phi_i \rangle |^2 dX} \quad (7)$$

$$f_{FSI} = \frac{\int N | \langle \chi_f^{(-)} | M^0 | \phi_i \rangle |^2 dX}{\int N | \langle \phi_f | M^0 | \phi_i \rangle |^2 dX} \quad (8)$$

$$f_{tot} = f_{FSI} \cdot f_{ISI} \quad (9)$$

where $dX = dqd\Omega_\eta d\Omega_1$ and N contains all of the kinematic factors in Eq.(2). ϕ_i and ϕ_f are plane waves. Clearly these factors measure the importance of the pp distortion in the η production. The initial distortion factor f_{ISI} (dotted curve) is mainly due to the pp interaction in the 3P_0 channel. It reduces the magnitude of the cross sections by about 40 percent at all energies considered. On the other hand, the final distortion f_{FSI} (dashed) drastically increases the cross section as the energy approaches the threshold. This is due to the formation of a quasi-bound pp state in the 1S_0 channel at very low energies. The total distortion f_{tot} increases the plane-wave cross sections by a factor of about 1.5 at energies close to the threshold, but reduces the cross section at higher energies. Clearly, the initial and final state interactions play nontrivial roles in determining the calculated cross sections. This is however well known

from many nuclear reaction calculations using distorted-wave impulse approximation[11]. The results shown in Fig.2 already distinguish our work from all previous works in which the initial pp distortion at such high energies is either neglected[3] or evaluated[1,2,5] by using a NN potential which is only valid at low energies. In Ref.[4], the initial and final pp distortions are both neglected.

From the definitions Eqs.(7)-(9), we obviously can write Eq.(1) as

$$\sigma_{tot} = f_{tot}\sigma_{tot}^0 \quad (10)$$

where σ_{tot}^0 can be calculated from Eqs.(1)-(5) except that the distorted waves $\chi^{(\pm)}$ in Eq.(3) are replaced by the plane waves ϕ . We have found that the calculated distortion factor f_{tot} is rather insensitive to the detail of the production operator M^0 as far as it is of the range of nuclear force. In actual calculations, we calculate f_{tot} from the simple σ -exchange mechanism. Eq.(10) is then used in the calculation with the full complexities of Eq.(5) included in the plane-wave calculation of σ_{tot}^0 .

Before we discuss our results, it is necessary to point out that the relative phase between the πN , ηN and σN channels can not be fixed within the unitary multi-channel, multi-resonance model[6,7]. To be specific, we therefore choose $(\pi N \rightarrow \eta N)/(\eta N \rightarrow \eta N) \propto -1$ according to the SU(3) quark model of $N^*(S_{11}) \rightarrow \pi N, \eta N$ developed by Arima et. al[12]. However, the phase of the $\sigma N \rightarrow \eta N$ relative to other transition amplitudes can not be fixed within the phenomenological approach we are taking. We therefore present results with both + and - relative signs between $\sigma N \rightarrow \eta N$ and $\pi N \rightarrow \eta N$ amplitudes.

We first compare the contributions from the π -exchange and η -exchange. Their contributions are the full thin line and the full thicker lines in Fig.3. In contrast to all previous works[1-5], they are comparable. The origin of this is that the ηN scattering length determined in the unitary, multi-channel, multi-resonance model(see Table I of Ref.[7]) is about 0.88 which is considerably

larger than the value ≤ 0.55 used in previous calculations[1–5]. This important difference was mainly due to the inclusion of multi-resonance and non-resonant background interaction in the fit to the data. This was fully discussed in Ref.[7].

The solid curve in Fig.3 is obtained from our calculation with only π - and η -exchange. There is no adjustable parameters in this calculation. By including the σ -exchange, we obtain the dashed and dotted curves. The difference between them is due to uncertainty of the phase of the $\sigma N \rightarrow \eta N$ transition relative to the $\pi N \rightarrow \eta N$ transition. Clearly, the data can be described within the theoretical uncertainty of the present approach.

In conclusion, we have shown that the near threshold $pp \rightarrow \eta pp$ reaction can be described with no adjustable parameters by using a meson-exchange model mediated by the exchange of π, η mesons. The use of the unitary multi-channel, multi-resonance model to generate the $\pi N, \eta N \rightarrow \eta N$ amplitudes is essential. The initial and final pp distortions calculated from realistic NN models are also shown to be very important in achieving the agreement with the data. The two- π exchange, simulated by a σ -exchange, is found to be of some importance. To quantify this mechanism, it is necessary to investigate the corresponding mechanism in other η production reactions such as the photoproduction of η meson on the nucleon. Our effort in this direction will be reported elsewhere.

References

- [1] J.F. Germond and C. Wilkin, *J. Phys. G* 15 (1989) 437.
- [2] J.F. Germond and C. Wilkin, *Nucl. Phys. A* 518 (1990) 308.
- [3] J.M. Laget, F. Wellers and J.F. Lecolley, *Phys. Lett. B* 257 (1991) 254.
- [4] T. Vetter, A. Engel, T. Biró and U. Mosel, *Phys. Lett. B* 263 (1991) 153.

- [5] C. Wilkin, Phys. Rev. C 47 (1993) R938.
- [6] M. Batinić, I. šlaus, A. švarc, and B.M.K. Nefken, Phys. Rev. C51(1995)2310
- [7] M. Batinić, šlaus, and A. švarc, Phys. Rev. C52(1995)2188
- [8] R. Machleidt, page 189, Vol.19, Advances in Nuclear Physics, edited by J.W. Negele and E.Vogt, Plenum Press(1989)
- [9] T.-S. H. Lee, Phys. Rev. C29(1984)195; T.-S. H. Lee and A. Matsuyama, Phys. Rev. C36(1987)1459
- [10] Particle Data Group, J.J. Hernandez et al., Review of Particle Properties, Phys. Lett. B239(1990)Vol.27
- [11] Herman Feshbach, Theoretical Nuclear Physics: Nuclear Reactions, John Wiley and son(1992)
- [12] M. Arima, K. Shimizu, and K. Yazaki, Nucl. Phys. A543(1992)613
- [13] V. Flamino et al, Compilation of cross sections, report CERN-HERA 79-03 (1979).
- [14] A.M. Bergdolt et al, Phys. Rev. D 48 (1993) R2969.
- [15] A. Taleb, thesis Nov 94, Univ. L. Pasteur de Strasbourg.
- [16] E. Chiavassa et al, Phys. Lett. B 322 (1994) 270.
- [17] H. Calén et al, Uppsala University preprint TSL/ISV-95-0124, ISSN 0284 - 2769 August 1995.

Figure captions

Fig. 1.

The Feynman diagram describing our process. The description of the variables is given in the text.

Fig. 2.

The values for the ISI and FSI distortion factors in the relevant energy range. The exact definitions are given in the text.

Fig. 3.

The Comparison of near threshold experimental results for the $pp \rightarrow pp\eta$ process with the predictions of our model. The meaning of each line is given in the legend of the Figure.

Fig. 1

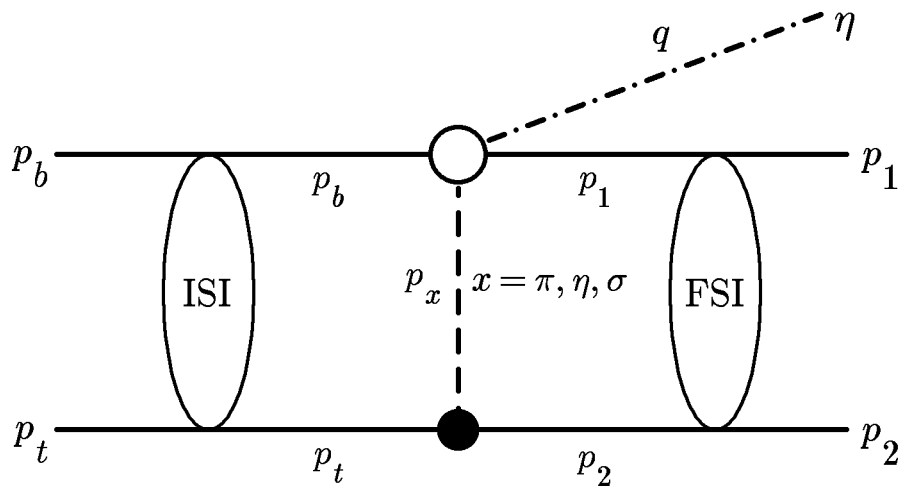


Fig. 2

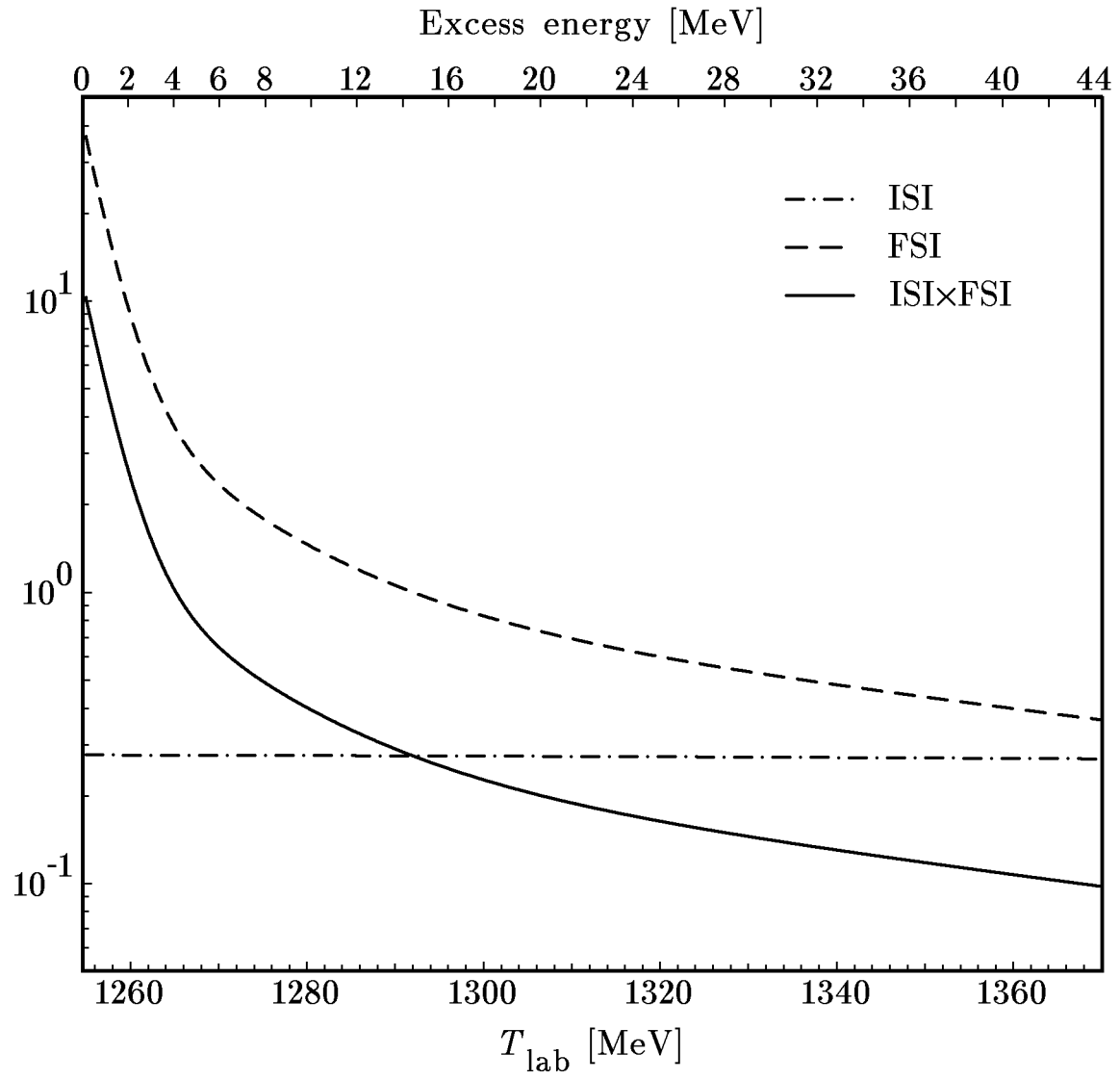


Fig. 3

